Stage-number dependence of intercalated species for fluorosilicate graphite intercalation compounds: pentafluorosilicate vs. hexafluorosilicate

Hiroki Yamamoto, Kazuhiko Matsumoto,* Rika Hagiwara

Graduate School of Energy Science, Kyoto University, Yoshida, Sakyo-ku, Kyoto 606-8501, Japan

**Corresponding author*. Tel: +81-75-753-4817. E-mail: k-matsumoto@energy.kyoto-u.ac.jp (K. Matsumoto)

Abstract

Most intercalated ions ever reported for graphite intercalation compounds (GICs) are singly charged, and the number of reports on GICs with doubly charged ions is limited. For fluorosilicate complex anions, only the intercalation of SiF_5^- was reported as stage-2 GICs, although SiF_6^{2-} is more commonly known in inorganic compounds. In the present study, chemical states of fluorosilicate GICs (SiF_y-GICs) are investigated along with the change in stage numbers. Syntheses of SiF_y-GICs at various stage numbers (the mixtures of stage-5 and -4, stage-4 and -3, stage-3 and -2, and stage-3 and -2) clarify that SiF_y-GICs at a low stage number have a larger gallery height than those at higher stage numbers. In addition, reactions of SiF_y-GICs with PF_5 formed PF_6-GICs with large weight increase and stage-number decrease, which cannot be explained by the substitution of SiF_4 with PF_5 to intercalate PF_6^-. The model that SiF_6^{2-} and SiF_5^- are present in GICs at high and low stage numbers, respectively (SiF_6^{2-} for stage-n ($n \geq 3$) and SiF_5^- for stage-2), can explain this phenomenon, suggesting intercalation of SiF_6^{2-} into graphite for the first time and stage-number dependency of intercalated species for fluorosilicate GICs.

Keywords

graphite intercalation compound; fluorocomplex anions; multiply charged anions; pentafluorosilicate; hexafluorosilicate; hexafluorophosphate

Graphical abstract

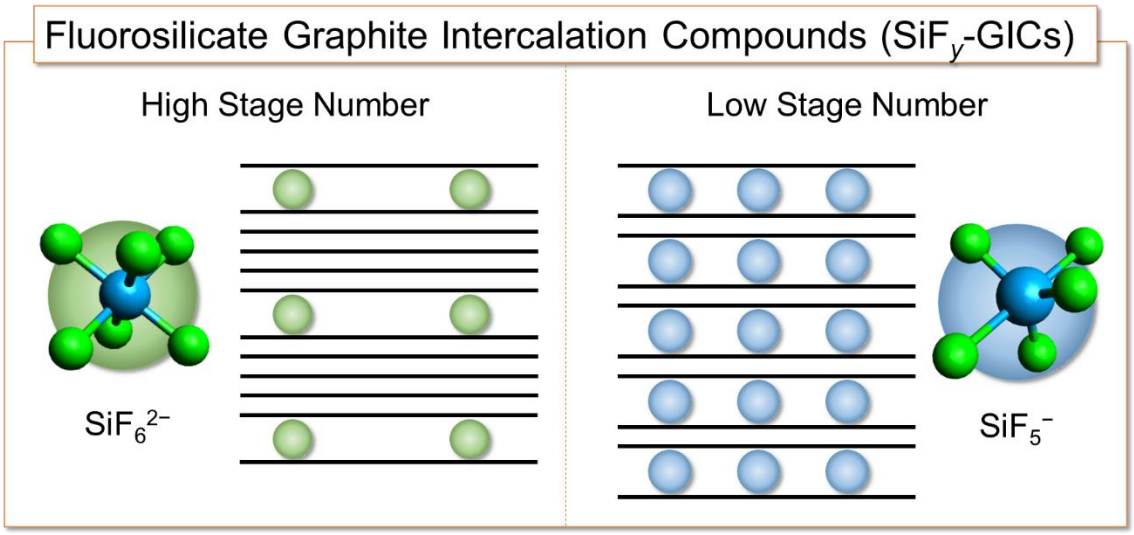

1. Introduction

Graphite is one of the carbon allotropes with a layered structure of so-called graphene consisting of a hexagonal skeleton of sp^2 hybridized carbon atoms. The graphene layers weakly interact with each other by the van der Waals interaction in graphite. This unique structure allow various chemical species to be intercalated into the space between the layers to form graphite intercalation compounds (GICs) [1,2]. There are some known and possible applications of GICs, such as negative electrodes for lithium ion batteries [3,4], precursors of exfoliated graphite [5,6], and electrical conductive materials [7,8].

The formation of GICs is accompanied by the redox reactions between graphite and a chemical species, resulting in intercalation of cations or anions. Donor- and acceptor-type GICs are formed by reduction and oxidation of graphite, along with intercalation of cations and anions, respectively. A variety of intercalates are known such as Li^+, K^+, and Cs^+ for donor-type, and $AlCl_4^-$, AsF_6^-, and $N(SO_2F)_2^-$ for accepter-type GICs, partly in view of applications as electrodes for energy storage devices [1,9-11]. Neutral molecules can be co-intercalated together with cations and anions for weakening electrostatic repulsion among them. For donor-type GICs, organic molecules such as furan and epoxyethane can be co-intercalated into K-GICs to form ternary GICs [12]. Intercalation of organic solvents into graphite together with Li^+ is also known, related to GIC formation for lithium ion batteries [13,14]. For AsF_6-GICs, reaction of graphite with AsF_5 brings co-intercalation of AsF_3 and AsF_5 neutral molecules. However, release of the neutral molecules under vacuum was confirmed, and the stability of the neutral molecules is still controversial [15,16].

One of the interesting structural properties for GICs is the staging structure, where intercalates are periodically present between graphene layers; the staging structure with

intercalates in every *n*th graphene layers is called stage-*n*. Whereas the Rüdorff–Hoffmann model is a classical and simple staging model, the Daumas–Hérold model is known to explain better how the stage number changes accompanied by the increase of the quantity of intercalates [1,17,18]. The characteristic arrangement of intercalates in the graphite gallery are also great interests for theoretical researchers and have been investigated from kinetic aspects using various computational methods [19-22]. For the structure of the stage-*n* GICs, the following equation (Eq. (1)) is known to be established:

$$I_c = l \cdot d_{00l} = d_s + (n-1) \cdot d_g = (d_i + d_g) + (n-1) \cdot d_g \quad (1)$$

where I_c is the repeat distance of the GICs along the *c*-axis (identity period), *n* is the stage number of GICs, d_{00l} is the *d* spacing of the 00*l* diffraction, d_s is the gallery height, d_g is the interplanar distance of pure graphite ($d_g \approx 3.35$ Å), and d_i is the ion height along the *c*-axis. The stage number is related to properties of GICs. For example, the electric conductivity along the *ab*-plane of the graphene layer for AsF_6-GICs is the largest for stage-2, although the quantity of intercalates for stage-2 is smaller than that of stage-1 [7,23]. Therefore, exploring the properties and structure along with the stage number is an interesting subject in this field.

Almost all the intercalated ions in the previous literature are singly charged such as Li^+, K^+, AsF_6^-, and SbF_6^- [1]. There are only a limited number of papers reporting the presence of doubly charged discrete ions, including the GICs of Ca^{2+}, PbF_6^{2-}, SnF_6^{2-}, and GeF_6^{2-} [8,24,25]. For PbF_6^{2-} and SnF_6^{2-}, intercalation of singly charged anions of PbF_5^- and SnF_5^- was suggested in other previous papers [26,27]. The GeF_6^{2-} anion was suggested to be intercalated in the equilibrium with GeF_5^- under the presence of F_2 [25]. Therefore,

the intercalation of PbF_6^{2-}, SnF_6^{2-}, and GeF_6^{2-} is still under discussion. Within the tetrafluorides of the 14th-group elements, SiF_4 was not reported to be intercalated as SiF_6^{2-} although intercalation of SiF_5^- to form stage-2 SiF_5-GICs was reported before [28]. In the present study, chemical states of the intercalates and structures of GICs of fluorosilicate complex anions (SiF_y^{z-}) (SiF_y-GICs) are investigated by structural transformation along with the stage number change and reactivity with PF_5. Results are discussed based on the experimental data obtained by gravimetry, X-ray diffraction (XRD), and X-ray fluorescence (XRF) and infrared (IR) spectroscopies.

2. Results and discussion

2.1. Preparation of SiF_y-GICs at different stage numbers

Table 1 shows synthetic conditions of SiF_y-GICs by the reaction of graphite with SiF_4 in the presence of F_2. Structures of GICs were characterized by XRD measurements to determine their stage numbers, n. For many fluorocomplex-anion-GICs, the strongest and second strongest peaks can be indexed as $00n+1$ and $00n+2$ diffraction, respectively, due to the similar d_s for fluorocomplex anions to the c-cell constant of graphite [29,30]. Therefore, in the present study, n is determined by Eq. (2):

$$(n+1)\cdot d_{00n+1} = (n+2)\cdot d_{00n+2}\ (= I_c) \quad (2)$$

Eq. (2) can be arranged to Eq. (3) to evaluated n:

$$n = (2\cdot d_{00n+2} - d_{00n+1}) / (d_{00n+1} - d_{00n+2}) \quad (3)$$

The n should be integer ideally, and the number which is not integer suggests mixing of several stage numbers.

Fig. 1 (a), (b), (c), and (d) show XRD patterns of SiF_y-GICs formed under 0.1, 0.4, 1.0, and 2.5 atm of SiF_4 and F_2, respectively (No. 1, 2, 3, and 4 in Table 1). The diffraction data (see the caption of Fig. 1) provide n = 4.3, 3.4, 2.8, and 2.3 for (a), (b), (c), and (d), respectively, calculated by Eq. (3). Suppose these numbers mean stage mixing, they are regarded as the mixtures of stage-5 and stage-4 for (a), stage-4 and stage-3 for (b), and stage-3 and stage-2 for (c) and (d). These stage numbers are denoted as stage-[5+4], -[4+3], -$[3+2]_H$, and -$[3+2]_L$ for (a), (b), (c), and (d), respectively, in this study. The interesting feature of these patterns are the position of the 00n+2 diffraction peaks (the second strongest peaks) for (d) compared with (c). The second strongest peak of SiF_y-GICs is generally considered to shift to the higher angle along with the decrease of the stage number due to their peak positions above 26.5° (see Supplementary Data S.1. for the relation of XRD peak positions and stage numbers for GICs). This rule is applied for SiF_y-GICs at stage-[5+4], -[4+3], and -$[3+2]_H$, as is shown in Fig. 1 (a), (b), and (c). However, the second strongest diffraction peak for stage-$[3+2]_L$ is located at a smaller angle than that for stage-$[3+2]_H$ in spite of the smaller stage number (Fig. 1 (c) and (d)). This result suggests that the intercalated species are different between them and the size of the intercalate of (d) is larger than that of (a), (b), and (c). On the other hand, peaks suggesting in-plane structures are not observed unlike other GICs such as Li-GICs and AsF_6-GICs [16,31,32].

Table 1 Synthetic conditions of SiF_y-GICs by the reactions of graphite with SiF_4 in the presence of F_2.

No.	Gas pressure [atm]	Reaction time[a] [h]	Temp.[b] [K]	W_{before}[c] [mg]	W_{after}[c] [mg]	Product
1	SiF_4 : 0.1 F_2 : 0.1	48	298	510	565	SiF_y-GICs (stage-[5+4]) and graphite
2	SiF_4 : 0.4 F_2 : 0.4	24 24	298 348	228	268	SiF_y-GICs (stage-[4+3]) and graphite
3	SiF_4 : 1.0 F_2 : 1.0	44	298	1001	1292	SiF_y-GICs (stage-$[3+2]_H$))
4	SiF_4 : 2.5 F_2 : 2.5	24 24	298 323	396	541	SiF_y-GICs (stage-$[3+2]_L$))

[a]First and second lines for No. 2 and 4 mean reaction times in the first and second steps, respectively. [b]First and second lines for No. 2 and 4 mean reaction temperatures in the first and second steps, respectively. [c]W_{before} and W_{after} denote the weights before and after the reactions.

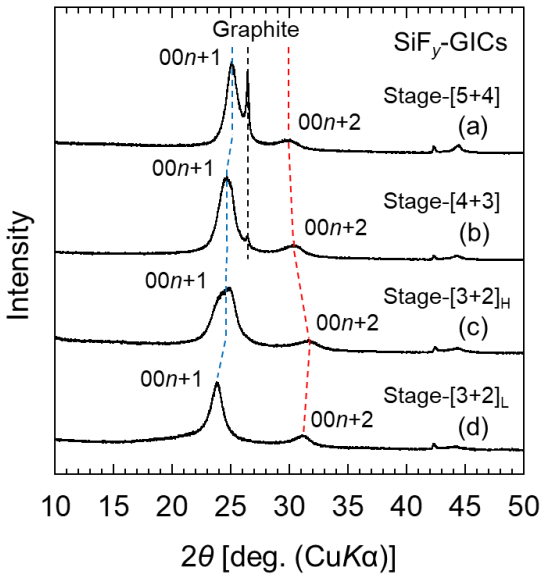

Fig. 1. XRD patterns of SiF_y-GICs at different stage numbers. Diffraction patterns, (a), (b), (c), and (d), correspond to the products formed by the reactions of graphite with 0.1, 0.4, 1.0, and 2.5 atm of SiF_4 and F_2, respectively (see Table 1 for synthetic conditions). The numbers in the brackets show the mixed stage numbers. Diffraction angles of the strongest and the second strongest peaks are 25.10° and 29.94° (d = 3.55 Å, and d = 2.98 Å) for (a), 24.74° and 30.50° (d = 3.60 Å, and d = 2.93 Å) for (b), 24.96° and 31.64° (d = 3.57 Å and d = 2.83 Å) for (c), and 23.85° and 31.17° (d = 3.73 Å and d = 2.87 Å) for (d).

2.2. Reactions of SiF_y-GICs with PF_5

The reactions of SiF_y-GICs with PF_5 provided crucial information to clarify the intercalates of SiF_y-GICs, and Table 2 shows their reaction conditions. These reactions proceed based on the stronger F^- affinity of PF_5 than that of SiF_4 because the stability of fluorocomplex anions-GICs almost depends on F^- affinity of parent fluorides [28]. Fig. 2

(a), (b), (c), and (d) shows XRD patterns of the products formed by the reactions of SiF_y-GICs (corresponding to Fig. 1 (a), (b), (c) and (d), respectively) with 1.0 atm of PF_5 at 298 K (No. 1, 2, 3, and 4 in Table 2), respectively. The diffraction data (see the caption of Fig. 2) provide n = 3.1, 2.1, 2.1, and 1.8 for (a), (b), (c) and (d), respectively, according to Eq. (3), indicating the formation of stage-3 for (a), stage-2 for (b), and stage-2 for (c). In the case of (d), the stage-1 compound seems to be contained in addition to the stage-2 compound because a shoulder peak at the lower angle is confirmed. Therefore, its stage number is denoted as stage-[2+1]. The gallery heights calculated by Eq. (1) are d_s = 7.53, 7.46, and 7.45 for (a), (b), and (c), respectively, which are similar to each other and close to d_s of PF_6-GICs reported [28].

One can recognize that the peaks ascribed to unreacted graphite in the XRD patterns of SiF_y-GICs at stage-[5+4] and -[4+3] (Fig. 1 (a) and (b)) disappear after their reactions with PF_5 (Fig. 2 (a) and (b)). As is known in previous works [28], PF_5 alone does not react with graphite due to its weak oxidation power unlike AsF_5 and SbF_5. Therefore, the reaction of graphite with PF_5 is considered to occur owing to the presence of SiF_y-GICs. The PF_6-GICs are first formed by the reactions of SiF_y-GICs with PF_5, and the PF_6-GICs were reacted with graphite by transfer of PF_6^- between them in the second step. A similar phenomenon was reported for AsF_6-GICs, where stage-1 AsF_6-GICs reacts with graphite to form stage-2 AsF_6-GICs [16].

It is noteworthy that the stage number decreases after the reactions of SiF_y-GICs with PF_5; stage-[5+4], -[4+3], -$[3+2]_H$, and -$[3+2]_L$ for SiF_y-GICs changed to stage-3, -2, -2, and -[2+1] for PF_6-GICs, respectively. Although the reactions of stage-2 SiF_5-GICs with PF_5 were investigated in a previous study, stage-2 PF_6-GICs were formed without the change of the stage number [28]. The substitution reaction of SiF_4 with PF_5 to intercalate

PF_6^- was confirmed in the previous study, but the decrease of the stage number in the present study cannot be explained solely by the substitution reaction, because it requires to fill the space in the gallery. This result is consistent with the weight change; as shown in Table 2, the increases of weight after the reactions are too large to be explained by the simple replacement of SiF_4 with PF_5.

Table 2 Reaction conditions of SiF_y-GICs with PF_5.[a]

No.	Starting GICs	W_{before}[b] [mg]	W_{after}[b] [mg]	W_{subst}[c] [mg]	Product
1	SiF_y-GICs (stage-[5+4]) and graphite	202	224	205	PF_6-GICs (stage-3)
2	SiF_y-GICs (stage-[4+3]) and graphite	156	182	160	PF_6-GICs (stage-2)
3	SiF_y-GICs (stage-$[3+2]_H$)	299	348	311	PF_6-GICs (stage-2)
4	SiF_y-GICs (stage-$[3+2]_L$)	201	221	211	PF_6-GICs (stage-[2+1])

[a]The reactions were performed overnight at 298 K under the PF_5 pressure of 1.0 atm. [b]W_{before} and W_{after} denote the weights before and after the reactions. [c]W_{subst} denotes the weight after the reaction when the substitution of SiF_4 with PF_5 to intercalate PF_6^- is assumed to occur.

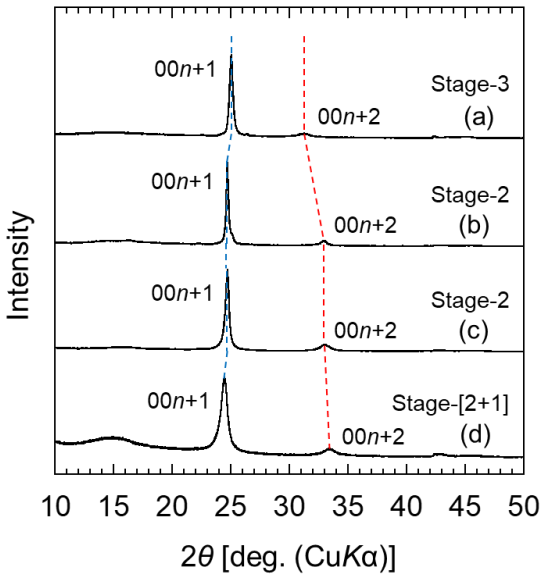

Fig. 2. XRD patterns of PF_6-GICs at different stage numbers. Diffraction patterns, (a), (b), (c) and (d), correspond to the products formed by the reactions of SiF_y-GICs at stage-[5+4], -[4+3], -$[3+2]_H$, and -$[3+2]_L$ with 1.0 atm of PF_5 at 298 K (see Table 2 for reaction conditions). The numbers in the bracket show the mixed stage numbers. Diffraction angles for the strongest and the second strongest peaks are 25.03° and 31.24° (d = 3.56 Å and 2.86 Å) for (a), 24.70° and 32.96° (d = 3.60 Å and 2.72 Å) for (b), 24.72° and 33.03° (d = 3.60 Å and 2.71 Å) for (c), and 24.46° and 33.38° (d = 3.64 Å and 2.68 Å) for (d).

2.3. Confirmation of conversion of SiF_y-GICs to PF_6-GICs

Substitution of SiF_4 with PF_5 to intercalate PF_6^- was confirmed by XRF spectroscopy as shown in Fig. 3, regarding the reaction No. 4 in Table 2. As is shown in Fig. 3 (a), the XRF spectrum of the SiF_y-GIC has a peak at 1.739 keV corresponding to Si-*K*α. After its reaction with PF_5, as shown Fig. 3 (b), the peak for Si-*K*α almost disappears and a peak

at 2.013 keV, corresponding to P-*K*α, appears. The negligible Si content (the Si/P ratio < 1.0 at%) suggests complete substitution of SiF_4 with PF_5. Liberation of SiF_4 from SiF_y-GICs by the reaction with PF_5 was also confirmed by the IR analysis of the residual gas after the reaction (see Fig. S1).

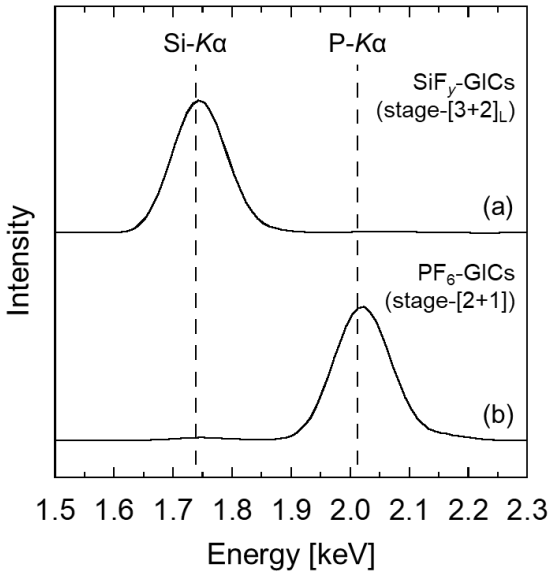

Fig. 3. XRF spectra of (a) SiF_y-GICs at stage-$[3+2]_L$ obtained by the reaction of graphite with 2.5 atm of SiF_4 and F_2 (No. 4 in Table 1) and (b) PF_6-GICs at stage-[2+1] obtained by reaction of SiF_y-GICs at stage-$[3+2]_L$ with PF_5 (No. 4 in Table 2). The Si/P ratio in the spectrum (b) < 1.0 at%.

2.4. Intercalated species in SiF_y-GICs

As mentioned above, the intercalated species for SiF_y-GICs is considered to change with the decrease of the stage number according to XRD measurements. In addition, reactions of SiF_y-GICs with PF_5 causes the decrease of the stage number and the large

weight increase which cannot be explained by the substitution of SiF_4 with PF_5. Two possible models are given below to explain these results. Table 3 shows compositions of SiF_y-GICs and PF_6-GICs calculated by the weight changes of the reactions in the two models (see Supplementary Data S.2 for detailed calculations).

The first model (Model 1) involves the change of the intercalated species; it is SiF_6^{2-} at high stage numbers and changes from SiF_6^{2-} to SiF_5^- with the decrease of the stage number (Fig. 4). It can be written in the following Eqs. (4) and (5) at high stage number, and (6) and (7) at low stage number:

At high stage numbers,

$$x\,C + SiF_4 + F_2 \rightarrow C_xSiF_6 \quad (4)$$

$$C_xSiF_6 + 2\,PF_5 \rightarrow 2C_{x/2}(PF_6) + SiF_4 \quad (5)$$

At low stage numbers,

$$x\,C + SiF_4 + 1/2\,F_2 \rightarrow C_xSiF_5 \quad (6)$$

$$C_xSiF_5 + PF_5 \rightarrow C_xPF_6 + SiF_4 \quad (7)$$

Here, SiF_6^{2-} and SiF_5^- could be co-intercalated in the same galleries. The increase of gallery height d_s for SiF_y-GICs from stage-[5+4] to -$[3+2]_L$ is well-explained by the change of the intercalate from SiF_6^{2-} to SiF_5^-. The pentagonal bipyramidal SiF_5^- (D_{3h}) provides different heights along *c*-axis, depending on its orientation in the gallery (see Fig. S2). The smallest height in GICs for SiF_5^- is achieved when F_{ax} and F_{ex} meet both of the upper and lower graphene layers (Fig. S2 (a); F_{ax} and F_{ex} are fluorine atoms at the axial and equatorial positions of SiF_5^-). It is considered to occur at low stage number, and

Eq. (1) provides the ion height along *c*-axis, d_i, of 4.60 Å from I_c of 11.30 Å for the stage-2 SiF_5-GICs in the previous literature [28]. In addition, the radius of F atom is calculated to be 1.23 Å from d_i (4.60 Å) and Si–F bond lengths of SiF_5^- (1.660 Å for $Si–F_{ax}$ and 1.622 Å for $Si–F_{eq}$ [33]). On the other hand, the smallest height of the octahedral SiF_6^{2-} (O_h) is achieved when its C_3-axis is located along the *c*-axis. When the radius of F atom is regarded to be the same in SiF_5- and SiF_6-GICs, d_i of SiF_6^{2-} is determined to be 4.42 Å (Si–F bond is 1.699 Å according to the literature) [34]. Deconvolution of the strongest peak in Fig. 1 (a) under the assumption that SiF_y-GICs at stage-[5+4] is the mixture of stage-5 and stage-4 SiF_6-GICs with d_i = 4.42 Å can fit the experimental data well (see Fig. S3 for the peak separation of XRD).

On the other hand, the weight change accompanied by the reactions of SiF_y-GICs with PF_5 can also be explained by Model 1. The number of PF_5 molecules to react with one SiF_6^{2-} is two, which means that SiF_6^{2-} brings more weight increase than SiF_5^- along with the change of intercalated anions (SiF_6^{2-} (142.1 g mol^{-1}) → $2PF_6^-$ (290 g $(2\ mol)^{-1}$); SiF_5^- (123.1 g mol^{-1}) → PF_6^- (145 g·mol^{-1})). Therefore, the change of intercalates from SiF_6^{2-} to SiF_5^- along with the decrease of the stage number can also rationalize the weight increase. The *y* value in SiF_y^{z-} based on weight change (Table 3) is nearly 6 for SiF_y-GICs at stage-[5+4] and -[4+3] and decreases from 6 to 5 accompanied by the decrease of the stage number, indicating the ratio of SiF_5^- to SiF_6^{2-} increases with decreasing the stage number. The SiF_y-GICs at stage-$[3+2]_H$ and -$[3+2]_L$, which contains stage-2 GICs, provide *y* lower than 6 (y = 5.6 and 5.2, respectively), suggesting that intercalate species are SiF_6^{2-} for stage-*n* ($n \geq 3$), and SiF_5^- for stage-2. Moreover, the *y* value of 5.2 for SiF_y-GICs at stage-$[3+2]_L$, which is close to 5, indicates that SiF_5^- is the major intercalates and it could cause the shift of 00*n*+2 peaks to lower angles compared with those of the other

SiF_y-GICs in the XRD pattern in Fig. 1.

The presence of SiF_6^{2-} is probably more favorable at high stage numbers in terms of the lattice energy. However, at low stage numbers, the repulsive forces between SiF_6^{2-} anions in different galleries or between positively charged adjacent graphene layers lead to the unstableness of doubly charged SiF_6^{2-}. Particularly for the stage-2 GICs, the repulsive forces between adjacent graphene layers are strong, because the graphene layers facing intercalates are next to each other, which is considered to be a driving force to change the intercalated species from SiF_6^{2-} to SiF_5^- for stage-2 GICs. Another possible reason for the unstableness of SiF_6-GICs at low stage numbers is the too-high charge density on the graphene sheets to compensate the doubly negative charge. Different gallery heights according to chemical species were also suggested for GeF_6^{2-} (d_s = 7.80 Å) and GeF_5^- (d_s = 8.23 Å) [25].

The other model (Model 2) is the case that only SiF_5^- is intercalated in SiF_y-GICs and intercalation of PF_5 neutral molecules occurs along with the substitution of SiF_4 with PF_5 to intercalate PF_6^- (see Fig. S4 for the schematic drawing of Model 2). The PF_5 molecules may interact with PF_6^- to form dinuclear complex anion such as $P_2F_{11}^-$, although its presence was not confirmed in previous works [35]. The reactions are described in the following Eqs. (8) and (9):

$$x\,C + SiF_4 + 1/2\,F_2 \rightarrow C_xSiF_5 \quad (8)$$

$$C_xSiF_5 + (1+w)\,PF_5 \rightarrow C_xPF_6(PF_5)_w + SiF_4 \quad (9)$$

Although the intercalated species is SiF_5^- for all the SiF_y-GICs, the different orientation of SiF_5^- in the gallery may cause the different gallery heights. The large weight increase

is explained by the co-intercalation of PF_5 neutral molecules along with PF_6^- (see Table 3 for the quantity of co-intercalated PF_5). However, this model has some unfeasible points. The reason for the orientation change along with the decrease of the stage number cannot be rationalized because the increase of d_s is generally unfavorable for the thermodynamic stability of GICs. Moreover, the presence of PF_5 molecules vacuum stable in the gallery is uncertain. Whereas there is a report about the presence of PF_5 molecules in PF_6-GICs (evacuation procedure is not mentioned) [35], a certain PF_5 dissociation pressure over PF_6-GICs was also suggested [28].

Table 3 Compositions of SiF_y-GICs and PF_6-GICs calculated by the weight changes in the syntheses of SiF_y-GICs and their reactions with PF_5 based on Model 1 and Model 2.

Stage number for SiF_y-GICs	Weight changes [g]		Composition[a]			
			Model 1		Model 2	
	Syntheses of SiF_y-GICs	Reactions with PF_5	SiF_y-GICs	PF_6-GICs	SiF_y-GICs	PF_6-GICs[b]
Stage-[5+4]	510 → 565	202 → 224	$C_{111}SiF_{6.1}$	$C_{53}PF_6$	$C_{95}SiF_5$	$C_{95}PF_6(PF_5)_{0.92}$
Stage-[4+3]	228 → 268	156 → 182	$C_{68}SiF_{6.1}$	$C_{32}PF_6$	$C_{58}SiF_5$	$C_{58}PF_6(PF_5)_{0.92}$
Stage-$[3+2]_H$	1001 → 1292	299 → 348	$C_{39}SiF_{5.6}$	$C_{24.4}PF_6$	$C_{35}SiF_5$	$C_{35}PF_6(PF_5)_{0.54}$
Stage-$[3+2]_L$	396 → 541	201 → 221	$C_{29}SiF_{5.2}$	$C_{24.2}PF_6$	$C_{28}SiF_5$	$C_{28}PF_6(PF_5)_{0.19}$

[a]Details to determine the compositions are given in Supplementary Data S2. [b]PF_5 may be stabilized by the interaction with PF_6^- to form dinuclear complex anion, $P_2F_{11}^-$ (its presence is just suggested in the previous study [35]).

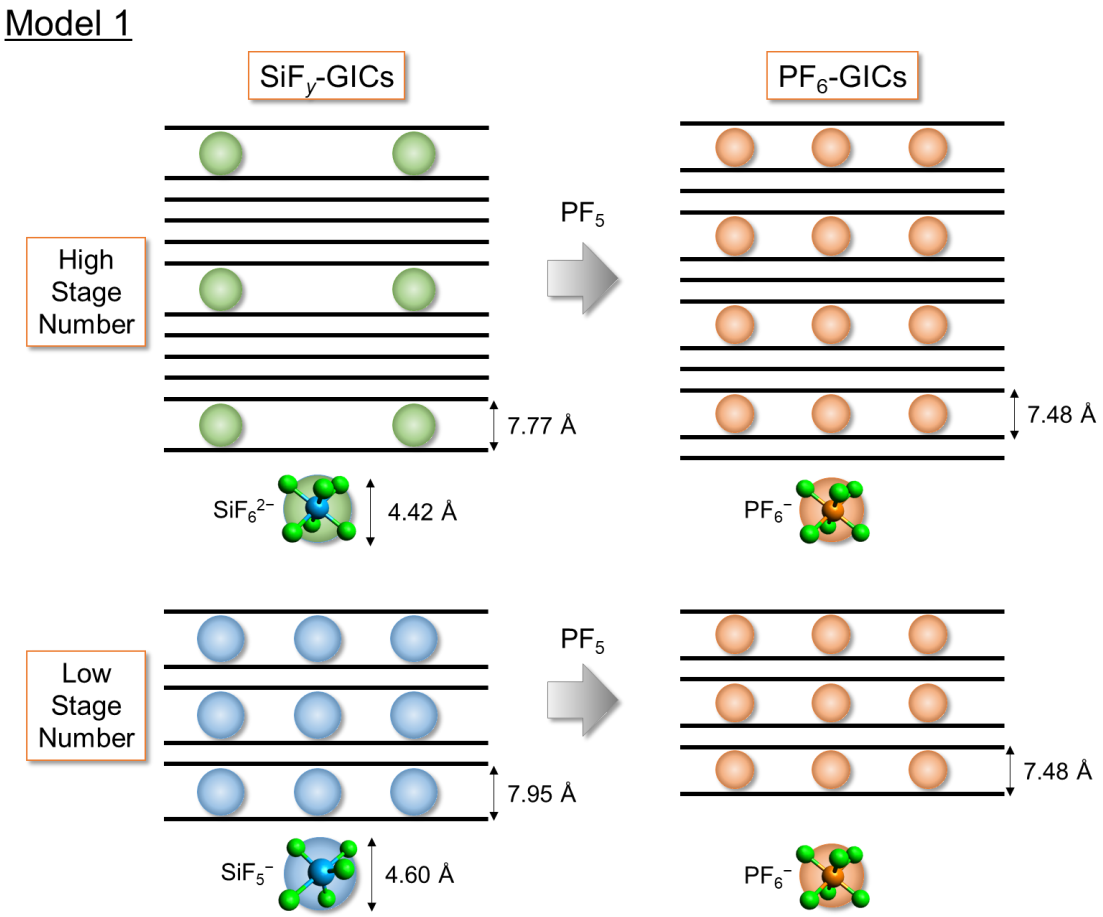

Fig. 4 A schematic drawing of Model 1 for the reactions of SiF_y-GICs with PF_5. The intercalated species of SiF_y-GICs changes depending on stage number; SiF_6^{2-}/SiF_5^- is intercalated into GICs at a high/low stage number (SiF_6^{2-} for stage-n ($n \geq 3$) and SiF_5^- for stage-2 are suggested). Sizes of SiF_6^{2-} and SiF_5^- are calculated based on their molecular and ionic structures and d_s of stage-2 SiF_5-GICs from literature (see Fig. S2 for details on the heights of SiF_5^- at different orientations) [28,33,34]. The number of ions in each gallery for SiF_6^{2-} is considered to be lower than that for SiF_5^-, because the distance between doubly charged SiF_6^{2-} anions is longer than that between singly charged SiF_5^- anions due to stronger repulsive forces. A schematic drawing of Model 2 is given in Fig. S4.

3. Conclusions

Exploring intercalation of doubly charged anions into graphene layers is not sufficiently studied, but important to extend possibilities of GICs. For the GICs of fluorosilicate anions, only the intercalation of SiF_5^- was reported in a previous work, although the chemical state of SiF_6^{2-} is more widely known. In the present study, SiF_y-GICs at various stage numbers (the mixtures of stage-5 and -4 (stage-[5+4]), stage-4 and -3 (stage-[4+3]), stage-3 and -2 (stage-$[3+2]_H$), and stage-3 and -2 (stage-$[3+2]_L$)) were synthesized and characterized by gravimetry, XRD, XRF, and IR, and their reactions with PF_5. The XRD measurements for SiF_y-GICs confirmed that SiF_y-GICs at stage-$[3+2]_L$ had a larger gallery height d_s than the others (stage-[5+4], -[4+3], and -$[3+2]_H$), suggesting that different chemical species were intercalated depending on the stage number. The reactions of SiF_y-GICs with PF_5 caused large weight increases and stage-number decreases cannot be explained only by the substitution reaction of SiF_4 with PF_5 to intercalate PF_6^-. The reaction of graphite with PF_5 was also confirmed in the presence of SiF_y-GICs despite the weak oxidation power of PF_5. Two possible models were proposed here to explain these observations. In Model 1, intercalated species was changed from SiF_6^{2-} to SiF_5^- with decreasing the stage number (SiF_6^{2-} for stage-n ($n \geq 3$) and SiF_5^- for stage-2 were suggested), which could explain the change of d_s along the large weight increases and decreases of the stage numbers by the reactions with PF_5. In Model 2, SiF_5^- was regarded as the only intercalated species, but this model suffered from several inconsistencies, and Model 1 was more plausible. Intercalation of multiply charged fluorocomplex anions of the third raw main group element and difference in intercalate species, depending on the stage number, were suggested for the first time in this study, which can make a significant impact on various chemistries related to GICs. Subsequent

theoretical and analytical studies in this field is expected near future.

4. Experimental

4.1 Apparatus and Materials

Volatile materials were handled in a reaction line made of stainless steel and PFA (tetrafluoroethylene-perfluoroalkylvinylether copolymer) [36]. Nonvolatile materials were handled under a dry Ar atmosphere in a glove box. A Ni reactor (100 cm^3 in volume) was used for a reaction with a total pressure above 2 atm. A PFA reactor (typically 100-200 cm^3 in volume) was used for a reaction with a total pressure of or below 2 atm. Silicon tetrafluoride (Mitsui Chemicals, Inc.), PF_5 (Kanto Denka Kogyo Co., Ltd.), and F_2 (Daikin Industries, Ltd.) were used as supplied. Synthetic graphite powder (Union Carbide Corporation, SP-1, 100μm) was dried at 300°C under vacuum for 1 day prior to use.

4.2. Preparation of SiF_y-GICs by the reaction of graphite with SiF_4 in the presence of F_2.

Reaction conditions are summarized in Table 1. Graphite was weighed and loaded in the PFA reactor or Ni reactor in the glove box.

For the syntheses of SiF_y-GICs under total pressures of SiF_4 and F_2 of or below 2 atm (No. 1, 2, and 3 in Table 1), the reactor was evacuated to remove Ar. SiF_4 and F_2 were introduced into the reactor though the reaction line up to the target pressure and kept it at the reaction temperatures during the reaction time. The SiF_4 and F_2 gases were added into the reactor once or twice during the reactions to supply the consumed gases. After the reaction, the reactor was cooled down to 298 K and the volatile gases were removed under

vacuum.

For the synthesis of SiF_5-GICs under total pressures of SiF_4 and F_2 higher than 2 atm (No. 4 in Table 1), the reactor was evacuated to remove Ar. SiF_4 and F_2 were introduced into the reaction line and condensed into the reactor by cooling the reactor with liquid nitrogen, which resulted in 2.5 atm of SiF_4 and F_2 (total pressure of 5.0 atm). After 24-hour reaction at 298 K, the reactor was warmed up to 323 K and kept for 24 h. Then, the reactor was cooled down to 298 K and the volatile gases were removed under vacuum.

4.3. Reactions of SiF_y-GICs with PF_5

Reaction conditions are summarized in Table 2. The SiF_y-GICs synthesized in Section 4.2 were weighed and loaded in a PFA reactor in the glove box. After the evacuation of Ar in the reactor, PF_5 was introduced into the reactor through the reaction line up to 1.0 atm at 298 K. After the reactions overnight, the volatile gases were removed at 298 K under vacuum through a soda lime chemical trap at first and though a cold trap cooled with liquid nitrogen for one day.

4.4. Analyses

XRD patterns were obtained in a Bragg-Brentano geometry at a scan speed of 1.0 deg s^{-1} using a Smartlab diffractometer (Rigaku Corp., Cu *K*α radiation, 40 kV-30 mA) equipped with a D-tex Ultra 250 Si-strip high speed detector. Air-sensitive materials were loaded in an airtight cell with Be windows in the glove box. XRF spectra were obtained with energy dispersive X-ray fluorescence analyzer (Rigaku Corp., EDXL3000) under a He flow atmosphere. IR spectra of gaseous samples were recorded with an ALPHA II spectrometer (Bruker Optics Laboratories, Inc.) at a resolution of 4 cm^{-1} in the

transmission mode using a airtight cell with AgCl windows.

Declaration of Competing Interest

The authors declare no conflict of interest.

Acknowledgments

This study was partly supported by Japan Society for the Promotion of Science (JSPS, KAKENHI Grant Number 19H04695).

AppendixA. Supplementary Data

References

[1] M.S. Dresselhaus, G. Dresselhaus, Intercalation compounds of graphite, Adv. Phys. 30(2) (1981) 139-326.

[2] M. Inagaki, Applications of graphite intercalation compounds, J. Mater. Res. 4(6) (1989) 1560-1568.

[3] D. Aurbach, B. Markovsky, I. Weissman, E. Levi, Y. Ein-Eli, On the correlation between surface chemistry and performance of graphite negative electrodes for Li ion batteries, Electrochim. Acta 45(1) (1999) 67-86.

[4] S.J. An, J. Li, C. Daniel, D. Mohanty, S. Nagpure, D.L. Wood, The state of understanding of the lithium-ion-battery graphite solid electrolyte interphase (SEI) and its relationship to formation cycling, Carbon 105 (2016) 52-76.

[5] A. Celzard, J.F. Marêché, G. Furdin, Modelling of exfoliated graphite, Prog. Mater

Sci. 50(1) (2005) 93-179.

[6] K. Matsumoto, D. Minori, K. Takagi, R. Hagiwara, Expansion of tetrachloroaluminate-graphite intercalation compound by reaction with anhydrous hydrogen fluoride, Carbon 67 (2014) 434-439.

[7] G.M.T. Foley, C. Zeller, E.R. Falardeau, F.L. Vogel, Room temperature electrical conductivity of a highly two dimensional synthetic metal: AsF_5-graphite, Solid State Commun. 24(5) (1977) 371-375.

[8] T.E. Weller, M. Ellerby, S.S. Saxena, R.P. Smith, N.T. Skipper, Superconductivity in the intercalated graphite compounds C_6Yb and C_6Ca, Nat. Phys. 1(1) (2005) 39-41.

[9] K. Beltrop, P. Meister, S. Klein, A. Heckmann, M. Grünebaum, H.-D. Wiemhöfer, M. Winter, T. Placke, Does Size really Matter? New Insights into the Intercalation Behavior of Anions into a Graphite-Based Positive Electrode for Dual-Ion Batteries, Electrochim. Acta 209 (2016) 44-55.

[10] M. Zhang, X. Song, X. Ou, Y. Tang, Rechargeable batteries based on anion intercalation graphite cathodes, Energy Storage Mater. 16 (2019) 65-84.

[11] Y. Kondo, Y. Miyahara, T. Fukutsuka, K. Miyazaki, T. Abe, Electrochemical intercalation of bis(fluorosulfonyl)amide anions into graphite from aqueous solutions, Electrochem. Commun. 100 (2019) 26-29.

[12] J. Jegoudez, C. Mazieres, R. Setton, Behaviour of the binary graphite intercalation compounds KC_8 and KC_{24} towards a set of sample organic molecules, Synth. Met. 7(1) (1983) 85-91.

[13] T. Abe, N. Kawabata, Y. Mizutani, M. Inaba, Z. Ogumi, Correlation Between Cointercalation of Solvents and Electrochemical Intercalation of Lithium into Graphite in Propylene Carbonate Solution, J. Electrochem. Soc. 150(3) (2003) A257.

[14] G.H. Wrodnigg, Ethylene Sulfite as Electrolyte Additive for Lithium-Ion Cells with Graphitic Anodes, J. Electrochem. Soc. 146(2) (1999) 470.

[15] Y. Yacoby, The measurement of intercalant vibrations using Raman and infrared spectroscopies, Synth. Met. 34(1) (1989) 437-442.

[16] F. Okino, S. Kawasaki, H. Touhara, Preparation and properties of graphite hexafluoroarsenates C_xAsF_6 --preparation of stage-2 $C_{28}AsF_6$ by the reaction of stage-1 $C_{14}AsF_6$ with graphite, Mol. Cryst. Liq. Cryst. 387(1) (2002) 185-189.

[17] W. Rüdorff, U. Hofmann, Über Graphitsalze, Z. Anorg. Allg. Chem. 238(1) (1938) 1-50.

[18] N. Daumas and A. Hérold, Notes des Membres et Correspontants et Notes Présentéesou Transmises par Leurs Soins, C. R. Acad. Sci. Ser. C., 268 (1969) 373-375.

[19] E.M. Gavilán-Arriazu, O.A. Pinto, B.A. López de Mishima, D.E. Barraco, O.A. Oviedo, E.P.M. Leiva, The kinetic origin of the Daumas-Hérold model for the Li-ion/graphite intercalation system, Electrochem. Commun. 93 (2018) 133-137.

[20] E.M. Gavilán-Arriazu, M.P. Mercer, O.A. Pinto, O.A. Oviedo, D.E. Barraco, H.E. Hoster, E.P.M. Leiva, Effect of Temperature on The Kinetics of Electrochemical Insertion of Li-Ions into a Graphite Electrode Studied by Kinetic Monte Carlo, J. Electrochem. Soc. 167(1) (2020) 013533.

[21] M.Z. Bazant, Theory of Chemical Kinetics and Charge Transfer based on Nonequilibrium Thermodynamics, Acc. Chem. Res. 46(5) (2013) 1144-1160.

[22] M. Chandesris, D. Caliste, D. Jamet, P. Pochet, Thermodynamics and Related Kinetics of Staging in Intercalation Compounds, J. Phys. Chem. C 123(38) (2019) 23711-23720.

[23] Y. Gotoh, K. Tamada, N. Akuzawa, M. Fujishige, K. Takeuchi, M. Endo, R.

Matsumoto, Y. Soneda, T. Takeichi, Preparation of air-stable and highly conductive potassium-intercalated graphite sheet, J. Phys. Chem. Solids 74(10) (2013) 1482-1486.

[24] Y. Hattori, M. Kurihara, S. Kawasaki, F. Okino, H. Touhara, Syntheses of tin and lead fluoride graphite intercalation compounds and the phase transition of the tin fluoride compound, Synth. Met. 74(1) (1995) 89-93.

[25] E.M. McCarron, Y.J. Grannec, N. Bartlett, Fluorogermanium(IV) salts of graphite. A system in equilibrium with elemental fluorine, J. Chem. Soc., Chem. Commun. (19) (1980) 890-891.

[26] H. Touhara, K. Kadono, H. Imoto, N. Watanabe, A. Tressaud, J. Grannec, Some novel graphite intercalation compounds with involatile fluorides: Intercalation mechanism and in-plane electrical conductivity, Synth. Met. 18(1) (1987) 549-554.

[27] L. Fournes, T. Roisnel, J. Grannec, A. Tressaud, P. Hagenmuller, H. Imoto, H. Touhara, Structural investigation and ^{119}Sn Mössbauer study of graphiteSnF_4 intercalation compound, Mater. Res. Bull. 25(1) (1990) 79-87.

[28] G.L. Rosenthal, T.E. Mallouk, N. Bartlett, Intercalation of graphite by silicon tetrafluoride and fluorine to yield a second-stage salt $C_{24}SiF_5$, Synth. Met. 9(4) (1984) 433-440.

[29] G. Schmuelling, T. Placke, R. Kloepsch, O. Fromm, H.-W. Meyer, S. Passerini, M. Winter, X-ray diffraction studies of the electrochemical intercalation of bis(trifluoromethanesulfonyl)imide anions into graphite for dual-ion cells, J. Power Sources 239 (2013) 563-571.

[30] X. Zhang, N. Sukpirom, M.M. Lerner, Graphite intercalation of bis(trifluoromethanesulfonyl) imide and other anions with perfluoroalkanesulfonyl substituents, Mater. Res. Bull. 34(3) (1999) 363-372.

[31] D. Billaud, F.X. Henry, M. Lelaurain, P. Willmann, Revisited structures of dense and dilute stage II lithium-graphite intercalation compounds, J. Phys. Chem. Solids 57(6) (1996) 775-781.

[32] F. Okino, N. Bartlett, Hexafluoroarsenates of graphite from its interaction with AsF_5, $AsF_5 + F_2$, and O_2AsF_6, and the structure of $C_{14}AsF_6$, J. Chem. Soc., Dalton Trans. (14) (1993) 2081-2090.

[33] D. Schomburg, R. Krebs, Structural chemistry of pentacoordinated silicon. Molecular structures of the pentafluorosilicate anion and the diphenyltrifluorosilicate anion, Inorg. Chem. 23(10) (1984) 1378-1381.

[34] R.P. Sharma, R. Bala, R. Sharma, U. Rychlewska, B. Warżajtis, First X-ray structure of hexaamminecobalt(III) salt with complex fluoroanion: Synthesis and characterization of $[Co(NH_3)_6]X{\cdot}SiF_6{\cdot}nH_2O$, where X=Cl, Br, I and NO_3 and crystal structure of $[Co(NH_3)_6]Cl{\cdot}SiF_6{\cdot}2H_2O$, J. Fluorine Chem. 126(6) (2005) 967-975.

[35] H. Selig, A.J. Leffler, The ^{31}P Resonance of PF_6^- and Related Subspecies Intercalated in Graphite as a Function of Temperature, Inorg. Chem. 32(4) (1993) 490-490.

[36] K. Matsumoto, R. Hagiwara, Elimination of AsF_3 from anhydrous HF using $AgFAsF_6$ as a mediator, J. Fluorine Chem. 131(7) (2010) 805-808.